Journal of Applied Mechanics and Technical Physics, Vol. 35, No. 5, 1994

LIGHT-INDUCED DRIFT OF A ONE-COMPONENT GAS IN A FLAT CHANNEL

V. G. Chernyak, I. V. Chermyaninov, E. A. Vilisova, and E. A. Subbotin

UDC 533.72:535.21

The phenomenon of bulk, light-induced drift (BLID), predicted in [1], consists in the fact that particles that are absorbing radiation in the form of a monochromatic traveling wave and are mixed with a buffer gas acquire directional motion. The possibility of BLID of a one-component gas under the condition that the excited and unexcited particles interact differently with the boundary surface — surface BLID — was substantiated in [2]. This mechanism was used in [3] to estimate the BLID hydrodynamic regime in channels.

Light-induced slippage of a one-component gas (a Knudsen layer) was calculated in [4, 5]. A new BLID mechanism was predicted, which can be called collisional, since it owes its existence to the difference between the collisional cross sections of excited and unexcited particles. Collisional BLID is possible only in a confined gas. It is analogous, in a certain sense, to diffusional slippage of an isotopic gas mixture. This mechanism was used in [6] for a numerical calculation of velocity and heat-flux profiles in a flat channel for certain values of the determining parameters.

In the present paper we give the results of a calculation of BLID for a one-component gas in a flat channel at arbitrary Knudsen numbers (Kn) with allowance for both the surface mechanism and the collisional mechanism. The main difficulty in such a calculation is associated with the need to solve the Boltzmann kinetic equation or models of it at intermediate Kn, which is the fundamental problem of the kinetic theory of gases. Here three methods are used to solve the kinetic equation with an approximating collision integral: the method of discrete ordinates, the integral–moment method, and the mixed integrodifferential–moment method. A comparison of the results obtained enables us to evaluate the efficacy of each method.

1. Statement of the Problem. Let us consider established motion of a one-component gas between parallel plates, located at $X = \pm d/2$, under the action of resonant optical radiation propagating along the channel in the direction of the Z axis. We assume the distance between the plates to be much less than their length and width, i.e., the gas's motion is one-dimensional.

We confine ourselves to the model of two-level particles, with the lower level n corresponding to the ground state and the upper level m to the excited state. Let the radiation frequency ω be close to the frequency ω_{mn} of the electron or vibrational–rotational m–n transition. Owing to the Doppler effect, only particles with velocities close to the resonant velocity v_r, which satisfies the condition $kv_r = \Omega = \omega - \omega_{mn}$ (k is the wave vector), interact with the radiation. The particles that have absorbed radiation alter the transportive collisional cross section. The absorbing gas can then be treated as a binary gas mixture, the particles in which have the same mass and different collision cross sections.

In this case, the distribution functions for excited (f_m) and unexcited (f_n) particles satisfy the system of two kinetic equations [7]

$$\begin{aligned} v_x \frac{\partial f_m}{\partial X} &= \frac{1}{2}\varkappa(v_z)\Gamma_m(f_n - f_m) - \Gamma_m f_m + S_m, \\ v_x \frac{\partial f_n}{\partial X} &= -\frac{1}{2}\varkappa(v_z)\Gamma_m(f_n - f_m) + \Gamma_m f_m + S_n. \end{aligned} \tag{1.1}$$

Here

$$\varkappa(v_z) = \frac{4|g_{mn}|^2\Gamma}{\Gamma_m[\Gamma^2 + (\Omega - kv_z)^2]}, \quad g_{mn} = \frac{E_0 d_{mn}}{2\hbar}; \tag{1.2}$$

Ekaterinburg. Translated from Prikladaya Mekhanika i Tekhnicheskaya Fizika, No. 5, pp. 3-13, September-October, 1994. Original article submitted November 10, 1993.

0021-8944/94/3505-0643$12.50

Γ_m is the frequency of radiative decay of the excited state; Γ is the uniform half-width of the absorption line; S_m and S_n are the Boltzmann collision integrals; E_0 is the amplitude of the electric field; d_{mn} is a matrix element of the dipole moment of the resonant n−m transition; $\varkappa(v_z)$ is the saturation parameter, characterizing the probability of stimulated transitions (it is proportional to the radiation intensity I); $\hbar$ is Planck's constant.

If the probability of stimulated transitions is low, which occurs at low radiation intensities, then the states of the components of the gas mixture are slightly out of equilibrium and the distribution functions can be written as small perturbations of Maxwellian distributions,

$$f_i = f_{i0}[1 + h_i(X, \mathbf{v})] \quad (i = n, m),$$
$$f_{i0} = n_{i0}\left(\frac{m_0}{2\pi k_B T}\right)^{3/2} \exp\left(-\frac{m_0 v^2}{2k_B T}\right) \tag{1.3}$$

(n_{i0} is the equilibrium number density of the i-th component, T is the gas temperature, and k_B is the Boltzmann constant).

We assume that the interatomic collisions are elastic. Here each collision frequency $\gamma_i = \gamma_{ii} + \gamma_{ij}$ (γ_{ii} and γ_{ij} are the effective frequencies of elastic collisions between particles of the i-th type and particles of the ith and jth types, respectively) are much higher than the frequency Γ_m of radiative decay, i.e., $\Gamma_{mi} = \Gamma_m/\gamma_i \ll 1$.

The kinetic equations (1.1), linearized with respect to the perturbation functions h_i and the parameters Γ_{mi}, using second-order approximating collision integrals in McCormack's form [8], after being made dimensionless take the form

$$c_x \frac{\partial h_i}{\partial x} = \delta_i\left\{\frac{1}{2}\varkappa(c_z)\Gamma_{mi}\left(\frac{n_{j0} - n_{i0}}{n_{i0}}\right) + 2c_z[u_i - \varphi_{ij}^{(1)}(u_i - u_j)]\right.$$
$$\left. + 4c_x c_z[(1 - \varphi_{ii}^{(3)} + \varphi_{ii}^{(4)} - \varphi_{ij}^{(3)})\pi_{ixz} + \varphi_{ij}^{(4)}\pi_{jxz}] - h_i\right\}, \quad (i, j) = n, m, \quad i \neq j, \tag{1.4}$$

where

$$x = \frac{X}{d}, \quad \delta_i = \gamma_i \frac{d}{\bar{v}}, \quad \bar{v} = \left(\frac{2k_B T}{m_0}\right)^{1/2}, \quad \mathbf{c} = \frac{\mathbf{v}}{\bar{v}},$$
$$\varphi_{ij}^{(n)} = \frac{\nu_{ij}^{(n)}}{\gamma_i}, \quad u_i = \frac{U_i}{\bar{v}} = \int c_z E h_i d\mathbf{c}, \tag{1.5}$$
$$\pi_{ixz} = \frac{P_{ixz}}{2p_i} = \int c_x c_z E h_i d\mathbf{c}, \quad E = \pi^{-3/2}\exp(-c^2);$$

U_i, P_{ixz}, and p_i are the partial velocity, partial stress tensor, and partial pressure of the ith component, respectively; expressions for the frequencies $\nu_{ij}^{(n)}$ in terms of Chapman−Cowling Ω integrals have been given in [8]; δ_i is the rarefaction parameter, inversely proportional to Kn.

We confine ourselves to the consideration of elastic collisions of atoms with the surface and we use a specular−diffuse model of the boundary conditions, in accordance with which a fraction ε_i of particles of the ith type are scattered diffusely by the channel walls while a fraction $(1 - \varepsilon_i)$ are scattered specularly. The boundary conditions for the perturbation functions, linearized with allowance for (1.3), are written in the form

$$h_i(x = \mp 1/2, c_x \gtrless 0) = \varepsilon_i \nu_{ir} + (1 - \varepsilon_i)h_i(x = \mp 1/2, c_x \lessgtr 0). \tag{1.6}$$

Here $\nu_{ir} = (n_{ir} - n_{i0})/n_{i0}$ is the perturbation of the number density n_{ir} of particles of the ith type scattered diffusely; ε_i is the fraction of diffusely scattered particles ($\varepsilon_m \neq \varepsilon_n$ in this case).

If the channel surfaces have the same accommodation properties, the following symmetry conditions are obvious:

$$h_i(x = \mp 1/2, c_x \lessgtr 0) = h_i(x = \pm 1/2, c_x \gtrless 0). \tag{1.7}$$

It is of the greatest interest to calculate the macroscopic gas flux averaged over the channel cross section, which is determined by

$$J = J_m + J_n = \bar{v}\int_{-1/2}^{+1/2}(n_n u_n + n_m u_m)dx. \tag{1.8}$$

An important consequence of the assumption of a low probability of stimulated transitions is that the density of excited particles is much lower than the density of unexcited ones. One small parameter $(n_m/n_n) << 1$ has thus appeared in the theory. It is therefore appropriate to estimate all of the quantities in the kinetic equations (1.4) and to retain only those of first order with respect to the small parameter n_m/n_n.

If the excited and unexcited particles had the same collision cross sections and interacted in the same way with the channel surface, then BLID would be absent, i.e.,

$$n_n U_n + n_m U_m = 0.$$

Moreover, from the law of conservation of momentum it follows that the tensor of total shear-stress in the gas vanishes [see Eqs. (4.1) and (4.2)]:

$$n_n \pi_{nxz} + n_m \pi_{mxz} = 0.$$

It is thus obvious that

$$(u_n, \pi_{nxz}, h_n) \sim \frac{n_m}{n_n}(u_m, \pi_{mxz}, h_m).$$

For convenience in estimating all of the terms in the kinetic equations (1.4) and in future calculations, we introduce the functions

$$\Phi_i(x, c_x) = \frac{\alpha_i}{\pi\Gamma_{mi}\delta_i\varkappa}\int_{-\infty}^{+\infty}\int h_i(x, c)\exp(-c_y^2 - c_z^2)c_z dc_y dc_z, \tag{1.9}$$

where

$$\alpha_n = 1, \ \alpha_m = \frac{n_m}{n_n}, \ \varkappa = \pi^{-1/2}\int_{-\infty}^{+\infty} c_z \exp(-c_z^2)\varkappa(c_z)dc_z. \tag{1.10}$$

We also introduce new functions for the partial macroscopic velocities and partial shear stress:

$$\begin{aligned} w_i(x) &= \frac{\alpha_i U_i(x)}{\varkappa\Gamma_{mi}\delta_i} = \pi^{-1/2}\int_{-\infty}^{+\infty}\Phi_i(x, c_x)\exp(-c_x^2)dc_x, \quad i = m, n, \\ t_i(x) &= \frac{\alpha_i \pi_{ixz}(x)}{\varkappa\Gamma_{mi}\delta_i} = \pi^{-1/2}\int_{-\infty}^{+\infty}\Phi_i(x, c_x)\exp(-c_x^2)c_x dc_x. \end{aligned} \tag{1.11}$$

If we neglect terms of order n_m/n_n, then the kinetic equations (1.4) for the excited and unexcited states are converted, using Eqs. (1.9)-(1.11), to

$$c_x\frac{\partial\Phi_m}{\partial x} = \frac{1}{2} + \delta_m(1 - \varphi_{mn}^{(1)})w_m + 2\delta_m c_x(1 - \varphi_{mn}^{(3)})t_m - \delta_m\Phi_m; \tag{1.12}$$

$$\begin{aligned} c_x\frac{\partial\Phi_n}{\partial x} = &-\frac{1}{2} + \delta_n w_n + \delta_n\varphi_{nm}^{(1)}w_m + 2\delta_n c_x(1 \\ &- \varphi_{nn}^{(3)} + \varphi_{nn}^{(4)})t_n + 2\delta_m c_x\varphi_{mn}^{(4)}t_m - \delta_n\Phi_n. \end{aligned} \tag{1.13}$$

The fact that the radiation intensity is uniform over the channel cross section, so that $\varkappa$ does not depend on the x coordinate, is taken into account in Eqs. (1.12) and (1.13).

The boundary conditions and symmetry conditions for the functions Φ_i, with allowance for Eqs. (1.6), (1.7), and (1.9), have the form

$$\Phi_i(x = \mp 1/2, \ c_x \gtrless 0) = (1 - \varepsilon_i)\Phi_i(x = \mp 1/2, \ c_x \lessgtr 0); \tag{1.14}$$

$$\Phi_i(x = \mp 1/2, c_x \gtrless 0) = \Phi_i(x = \pm 1/2, \ c_x \gtrless 0). \tag{1.15}$$

In (1.14) we allowed for the fact that the first term on the right side of Eq. (1.6) makes no contribution to the macroscopic gas flux and therefore can be omitted.

We introduce the dimensionless quantity G, related to the macroscopic gas flux (1.8) by

$$G = \frac{2\pi^{1/2} J}{p\varkappa\Gamma_m d} = G_m + G_n,$$
$$G_i = 2\int_{-1/2}^{+1/2} dx \int_{-\infty}^{+\infty} \exp(-c_c^2)\Phi_i(x, c_x),\ i = m, n \tag{1.16}$$

($n = n_n + n_m$ is the total number of molecules per unit volume).

It is well known that the accommodation coefficients for gas motion in capillaries are close to unity [9], while the relative difference between the effective diameters of the excited (σ_m) and unexcited (σ_n) particles is small [10], i.e.,

$$(1 - \varepsilon_i) \ll 1,\ \Delta\sigma/\sigma_n \ll 1,\ \Delta\sigma = \sigma_m - \sigma_n. \tag{1.17}$$

The additional introduction of the small parameters (1.17) into the theory, after the appropriate linearization of the problem, enables us to separate the surface and collisional BLID mechanisms. The functions characterizing the velocity profile and the gas flow rate averaged over the channel cross section are converted to

$$w(x) = w_1(x)\Delta\varepsilon + w_2(x)\frac{\Delta\sigma}{\sigma_n},\ \Delta\varepsilon = \varepsilon_n - \varepsilon_m,$$
$$G = G_1\Delta\varepsilon + G_2\frac{\Delta\sigma}{\sigma_n}. \tag{1.18}$$

The kinetic coefficients G_1 and G_2, characterizing the contributions of the surface and collisional mechanisms, respectively, to BLID, depend only on the rarefaction parameter $\delta_n \equiv \delta$. Allowance for Eqs. (1.17) thus led to a considerable reduction in the number of calculation parameters to be given and thereby to a decrease in the volume of calculations.

Because of the inequalities (1.17) and $n_m \ll n_n$, we have

$$\theta = \frac{\delta_m}{\delta_n} = \frac{\gamma_{mn}}{\gamma_{nn}} = \frac{\sigma_{mn}^2}{\sigma_n^2} \approx 1 + \frac{\Delta\sigma}{\sigma_n},\ \sigma_{mn} = \frac{1}{2}(\sigma_m + \sigma_n),\ \delta_n \equiv \delta. \tag{1.19}$$

If the effective frequency of collisions of the n–n type is chosen in the form $\gamma_{nn} = p/\eta$ by analogy with the BGK model, and the viscosity coefficient is set equal to $\eta = \rho\bar{v}l\pi^{-1/2}$ (l is the mean free path of molecules in the gas), then the rarefaction parameter δ is related to the Knudsen number $Kn = l/d$ by the equation $\delta = \pi^{1/2}/(2Kn)$.

For any values of the parameters $\Gamma/(k_B\bar{v})$ and $\Omega/(k_B\bar{v})$, the quantity $\varkappa$ in (1.10) can be expressed in terms of the plasma function [11], while in the cases of nonuniform expansion ($\Gamma \ll k_B\bar{v}$) and uniform expansion ($\Gamma \gg k_B\bar{v}$), it has the form

$$\varkappa = \begin{cases} \dfrac{4\pi^{1/2}\Omega}{\Gamma_m}\left(\dfrac{|g_{mn}|}{k\bar{v}}\right)^2, & (|\Omega|, \Gamma) \ll k_B\bar{v}, \\ \dfrac{4k\bar{v}\Omega\Gamma}{\Gamma_m}\left(\dfrac{|g_{mn}|}{\Omega^2 + \Gamma^2}\right)^2, & (|\Omega|, \Gamma) \gg k_B\bar{v}. \end{cases} \tag{1.20}$$

Thus, solving the kinetic equations (1.12) and (1.13) with allowance for the boundary conditions (1.14) and the symmetry conditions (1.15) makes it possible to determine the surface component (w_1, G_1) and the collisional component (w_2, G_2) of BLID as a function of the rarefaction parameter δ.

2. Method of Discrete Ordinates (MDO). This method is based on the fact that the molecular velocity space is assumed to be discrete, i.e., it is assumed that the gas molecules can move only with certain fixed velocities. The set of discrete molecular velocities forms the nodes of the calculation grid.

Each of the equations (1.12) and (1.13) is approximated by a system of kinetic equations corresponding to the nodes c_{xq} of the calculation grid in velocity space. To solve those equations, in turn, we use a finite difference method in which partial derivatives with respect to the x coordinate are replaced by finite differences. As a result, we have calculation grids with nodes c_{xq} ($q = 1, 2, \ldots, N^c$) in velocity space and one with nodes x_k ($k = 0, 1, 2, \ldots, N^x$) in configuration space. The equations are then solved by successive approximations (iterations). The approximation order is denoted by the index p.

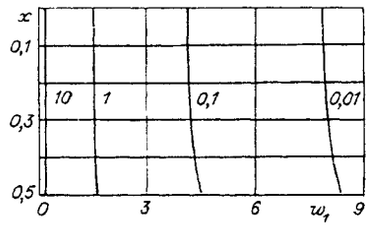

Fig. 1

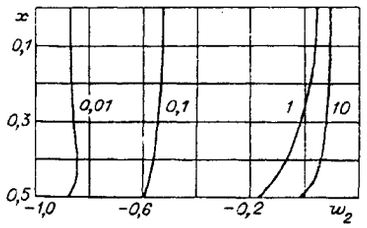

Fig. 2

For a molecular model of rigid spheres, we obtain difference schemes that approximate Eqs. (1.12) and (1.13) in the form

$$c_{xq}\frac{\Phi_{nk}^{(p)}-\Phi_{n,k-1}^{(p)}}{\Delta x}+\delta\Phi_{nk}^{(p)}=-\frac{1}{2}+\delta\left[w_{nk}^{(p-1)}+\frac{5}{6}\theta w_{mk}^{(p-1)}+\frac{2}{3}c_{xq}t_{mk}^{(p-1)}\theta\right],$$
$$c_{xq}\frac{\Phi_{mk}^{(p)}-\Phi_{m,k-1}^{(p)}}{\Delta x}+\delta\Phi_{mk}^{(p)}\theta=\frac{1}{2}+\delta\left[\frac{1}{6}\theta w_{mk}^{(p-1)}-\frac{2}{3}c_{xq}t_{mk}^{(p-1)}\theta\right], \tag{2.1}$$

where

$$w_{ik}^{(p)}=\pi^{-1/2}\sum_{q}^{N^c}\Phi_{ik}^{(p)}(x_k,c_{xq})\exp(-c_{xq}^2)\Delta c_x,\ i=n,m,$$
$$t_{mk}^{(p)}=\pi^{-1/2}\sum_{q}^{N^c}\Phi_{mk}^{(p)}(x_k,c_{xq})\exp(-c_{xq}^2)c_{xq}\Delta c_x; \tag{2.2}$$

$\Phi_{ikq}^{(p)}=\Phi_i(x_k, c_{xq})$ in the p-th approximation (i = n, m); Δx and Δc_x are the lengths of the partition segments of the respective calculation grid.

The boundary conditions (1.14) are transformed as follows:

$$\Phi_i^{(p)}(x=\mp 1/2,\ c_{xq}\gtrless 0)=(1-\varepsilon_i)\Phi_i^{(p-1)}\ (x=\mp 1/2,\ c_{xq}\lessgtr 0),\quad i=n,m. \tag{2.3}$$

It is seen from (2.1) that the perturbations of the distributions of m- and n-particles at the point (c_{xq}, x_k) are the functions

$$\Phi_{mk}^{(p)}=F_m(\Phi_{nk-1}^{(p)},\ w_{mk}^{(p-1)},\ t_{mk}^{(p-1)}),$$
$$\Phi_{nk}^{(p)}=F_n(\Phi_{nk-1}^{(p)},\ w_{nk}^{(p-1)},\ w_{mk}^{(p-1)},\ t_{mk}^{(p-1)}).$$

Taking certain (arbitrary, generally speaking) profiles of the macroscopic velocity and the stress tensor in the zeroth approximation (p = 0), and specifying the boundary conditions (2.3) at the surface, we can obtain the values of the perturbations Φ_n and Φ_m in any pth approximation at all nodes x_k:

$$\Phi_{mk}^{(p)}=\frac{\Phi_{mk-1}^{(p)}c_{xq}+\frac{\Delta x}{2}+\delta\Delta x\left(\frac{1}{6}w_{mk}^{(p-1)}\theta-\frac{2}{3}\theta c_{xq}t_{mk}^{(p-1)}\right)}{c_{xq}+\Delta x\delta\theta},$$
$$\Phi_{nk}^{(p)}=\frac{\Phi_{nk-1}^{(p)}c_{xq}-\frac{\Delta x}{2}+\delta\Delta x\left(w_{nk}^{(p-1)}+\frac{5}{6}\theta w_{mk}^{(p-1)}+\frac{2}{3}\theta c_{xq}t_{mk}^{(p-1)}\right)}{c_{xq}+\Delta x\delta}. \tag{2.4}$$

The iterations are continued until the difference between the perturbations in the (p — 1)-th and p-th approximations becomes less than some value specified in advance. The iteration accuracy in the present work was set at 10^{-6}.

For the zeroth approximation we chose the equilibrium state of the gas, in which

$$w_{ik}^{(0)}=0,\ t_{mk}^{(0)}=0,\ i=m,n,\ k=0,\ldots,N^x.$$

TABLE 1

δ	MDO		IMM		IDMM	
	G_1	$G_2 \cdot 10^{-1}$	G_1	$G_2 \cdot 10^{-1}$	G_1	$G_2 \cdot 10^{-1}$
0,01	8,006	−8, 623	8,016	−8,687	8,016	−8,686
0,04	5,633	−7,091	5,634	−7,091	5,634	−7,091
0,1	4,248	−5,438	4,227	−5,441	4,227	−5,441
0,4	2,475	−2,187	2,410	−2,222	2,410	−2,222
1	1,536	−0,115	1,441	−0,220	1,441	−0,220
2	0,962	0,886	0,868	0,711	0,868	0,713
3	0,694	1,127	0,614	0,931	0,613	0,935
4	0,539	1,121	0,472	0,956	0,470	0,963
5	0,438	1,105	0,382	0,918	0,380	0,928
6	0,368	1,037	0,321	0,860	0,318	0,874
10	0,223	0,775	0,196	0,642	0,191	0,666
15	0,150	0,576	0,133	0,468	0,126	0,498
20	0,114	0,450	0,101	0,365	0,094	0,397

We considered the range $[-5; 5]$ of dimensionless molecular velocities c_x. Terms with $|c_x| > 5$ make no significant contribution to (2.2). We used uniform and nonuniform grids in velocity space. The number of grid nodes was chosen so that increasing it changes the calculation result by no more than 0.1%. A uniform grid in velocity space was used for calculations with $\delta \leq 0.1$ and it contained $N^c = 1000$ nodes. A nonuniform grid consisting of 11 Gaussian nodes was convenient for calculations with $\delta > 0.1$. The segment $[-1/2; 0]$ along the x axis was divided into $N^x = 200$ parts for $\delta < 0.1$ and into $N^x = 300$ parts for $\delta \geq 0.1$.

We first calculated the values of the perturbation functions at nodes x_k of configuration space. Then from Eqs. (2.2) we found the profiles of macroscopic quantities, as well as the velocity averaged over the cross section.

In Figs. 1 and 2 we show BLID velocity profiles for different rarefaction parameters δ_n. The results of a calculation of G_1 and G_2 in Eq. (1.8) are given in Table 1.

3. Integral–Moment Method (IMM). Its essence consists in transforming the approximating kinetic equations into a closed system of integral equations for the moments of the distribution functions.

Equations (1.12) and (1.13), with allowance for the boundary conditions (1.14) and the symmetry conditions (1.15), are written in integral form, and are then transformed, using Eqs. (1.11), into a closed system of four integral equations for the partial velocities w_i and stresses t_i [12]:

$$w_i(x) = \int_{-1/2}^{+1/2} [A_i(s)K_{1i}(x, s) + B_i(s)K_{2i}(x, s)]ds; \tag{3.1}$$

$$t_i(x) = \int_{-1/2}^{+1/2} [A_i(s)K_{2i}(x, s) + B_i(s)K_{3i}(x, s)]ds, \; i = m, n. \tag{3.2}$$

Here

$$A_m(s) = \frac{1}{2\pi} + \delta_m \pi^{-1/2}(1 - \varphi_{mn}^{(1)})w_m(s),$$
$$B_m(s) = 2\delta_m \pi^{-1/2}(1 - \varphi_{mn}^{(3)})t_m(s),$$
$$A_n(s) = \pi^{-1/2}\left[-\frac{1}{2\pi^{1/2}} + \delta_n w_n(s) + \delta_m \varphi_{mn}^{(1)} w_m(s)\right],$$
$$B_n(s) = 2\pi^{-1/2}[\delta_n(1 - \varphi_{nn}^{(3)} + \varphi_{nn}^{(4)})t_n(s) + \delta_m \varphi_{mn}^{(4)} t_m(s)];$$

for $(1 - \varepsilon_i) \ll 1$ we have

$$K_{1i}(x, s) = I_{-1}(z_i) + (1 - \varepsilon_i)[I_{-1}(z_{1i}) + I_{-1}(z_{2i})],$$
$$K_{2i}(x, s) = I_0(z_i)\operatorname{sign}(x - s) + (1 - \varepsilon_i)[I_0(z_{1i}) + I_0(z_{2i})],$$
$$K_{3i}(x, s) = I_1(z_i) + (1 - \varepsilon_i)[I_1(z_{1i}) + I_1(z_{2i})],$$
$$z_i = \delta_i|x - s|, \; z_{1i} = \delta_i(x - s + 1), \; z_{2i} = \delta_i(s - x + 1),$$
$$I_n(x) = \int_0^\infty c^n \exp\left(-c^2 - \frac{x}{c}\right)dc.$$

The integral equations (3.1) and (3.2), of the second Fredholm type, can be solved by the Bubnov–Galerkin method [13]. In contrast to the MDO, it does not enable one to calculate profiles of velocity and stress, but with a felicitous choice of the test functions for the macroscopic parameters, it provides rapid convergence and satisfactory accuracy for the gas flow rate averaged over the channel cross section for any Kn.

The free terms in Eqs. (3.1) and (3.2) include the free-molecule values (Kn >> 1) of the velocity and stress. We therefore choose test functions that follow from the form of the macroscopic parameters in the hydrodynamic regime (Kn << 1):

$$\tilde{w}_i(x) = a_{1i} + a_{2i}x^2, \quad \tilde{t}_i(x) = a_{3i}x, \quad i = m, n \tag{3.3}$$

(a_{ki} are unknown constants).

Substituting Eqs. (3.3) into Eqs. (3.1) and (3.2) and requiring that the resulting expressions be orthogonal to each of the base functions [1 and x^2 for (3.1) and x for (3.2)], we obtain a system of algebraic equations for determining the constants a_{1i}, a_{2i}, and a_{3i}. Here the condition of orthogonality of two arbitrary functions f and g has the form

$$(f, g) = \int_{-1/2}^{+1/2} f(x)g(x)dx = 0.$$

If the constants a_{ki} are known, then the dimensionless gas flow rate is determined, with allowance for Eqs. (1.11), (1.16), and (3.3), from the expression

$$G = G_m + G_n, \quad G_i = 2\pi^{1/2}\left(a_{1i} + \frac{a_{2i}}{12}\right), \quad i = m, n. \tag{3.4}$$

Linearizing the resulting system of algebraic equations with respect to the small parameters (1.17), we find expressions for the kinetic coefficients G_1 and G_2 in (1.18).

Analytical expressions for G_1 and G_2 can be obtained only for large and small Kn.

1. Nearly free-molecule regime (Kn >> 1):

$$G_1 = -2\ln\delta, \quad G_2 = -1. \tag{3.5}$$

The fact that collisional BLID turns out not to vanish as $\delta \to 0$ is a consequence of the degenerate geometry of the problem (an infinitely wide channel). In fact, for total accommodation as $\delta \to 0$, the partial fluxes of unexcited and excited particles increase logarithmically without reaching the free-molecule values:

$$J_n \sim \ln\delta_n, \quad J_m \sim -\ln\delta_m = -\ln\delta_n - \ln\theta \approx -\ln\delta_n - \Delta\sigma/\sigma_n.$$

In summing the partial fluxes, the main terms of order $\ln \delta_n$ are retained and the collisional BLID turns out not to vanish. It is obvious that in the case of an actual channel geometry, such as for a cylindrical capillary [14], collisional BLID in the free-molecule regime will be absent.

2. Hydrodynamic regime with slippage (Kn << 1) for the model of rigid spherical molecules:

$$G_1 = \frac{6\pi^{1/2}}{5\delta}, \quad G_2 = \frac{9\pi^{1/2}}{20\delta}. \tag{3.6}$$

Numerical values of the kinetic coefficients G_1 and G_2 in the intermediate regime for the molecular model of rigid spheres are given in Table 1.

4. Integrodifferential-Moment Method (IDMM). The main difference from the IMM is that the profiles of partial velocities of the fluxes of excited and unexcited particles are described by the integral equations (3.1), while differential equations of transfer of the z component of the momentum must be obtained for the stress.

Multiplying Eqs. (1.12) and (1.13) by $\exp(-c_x^2)/\pi^{1/2}$ and integrating the resulting expressions over molecular velocity dc_x, with allowance for Eqs. (1.11) we have

$$\frac{\partial t_m}{\partial x} = \frac{1}{2} - \delta_m \varphi_{mn}^{(1)} w_m; \tag{4.1}$$

$$\frac{\partial t_n}{\partial x} = -\frac{1}{2} + \delta_m \varphi_{mn}^{(1)} w_m. \tag{4.2}$$

Note that the law of conservation of momentum, $t_m + t_n = 0$, follows from (4.1) and (4.2), i.e., the total shear-stress tensor vanishes.

The integral equations (3.1) and the differential equations (4.1) and (4.2) thus form a closed system determining the partial velocity $w_i(x)$ and partial stress $t_i(x)$.

In such an approach, using the Bubnov–Galerkin method, it is sufficient to approximate only the velocities $w_i(x)$, while the stress is determined from (4.1) and (4.2). If Eqs. (3.3) are taken as the test functions for $w_i(x)$, then, integrating (4.1) and (4.2) with allowance for the fact that there is no stress at the channel axis [$t_i(x = 0) = 0$], we obtain

$$\tilde{t}_m = -\tilde{t}_n = \left(\frac{1}{2} - \delta_m \varphi_{mn}^{(1)} a_{1m}\right) x + \frac{1}{3} a_{2m} x^3. \tag{4.3}$$

Substituting the approximations (3.3) for $w_i(x)$ and (4.3) for $t_i(x)$ into the integral equations (3.1) and requiring that the resulting expressions be orthogonal to each base function (1, x^2), we obtain a system of algebraic equations for the four unknown constants a_{1i} and a_{2i} (instead of the six in the IMM).

The quantity G, characterizing the gas flow rate, is determined from Eqs. (3.4).

The results of a numerical calculation of the kinetic coefficients G_1 and G_2 for different rarefaction parameters δ in the molecular model of rigid spheres are given in Table 1.

The analytical expressions for G_1 and G_2 in the free-molecule regime coincide with (3.5), while in the hydrodynamic regime with slippage, in the model of rigid spherical molecules, they have the form

$$G_1 = \left(\frac{39\pi^{1/2}}{35} - \frac{12}{35\pi^{1/2}}\right)\frac{1}{\delta}, \quad G_2 = \left(\frac{3}{5\pi^{1/2}} + \frac{51\pi^{1/2}}{140}\right)\frac{1}{\delta}. \tag{4.4}$$

A comparison of (4.4) with (3.6) yields a discrepancy of 18% for G_1 and 21% for G_2.

5. Discussion. In Table 1 we give the results of the numerical calculation of the kinetic coefficients G_1 and G_2 for intermediate rarefaction parameters δ by three methods: the MDO, IMM, and IDMM. The error in calculations by the MDO was less than 1%, which enables us to use those results to evaluate the accuracy of calculations by the IMM and IDMM. The main advantage of the latter two methods consists in the fact that they do not require calculations of local values of the macroscopic parameters. The IMM and IDMM are therefore more economical and require considerably less computer time than the MDO. At the same time, their accuracy depends on the choice of the approximating expressions for the macroscopic parameters [for the partial velocities and partial shear stress (3.3)].

It follows from Table 1 that the results obtained by the different methods are in satisfactory agreement for $\delta \leq 1$. For intermediate values of the rarefaction parameter δ, however, the maximum error of the IMM and IDMM results is about 20%. Reducing this error requires the use of a higher approximation of the Bubnov–Galerkin method to solve the system of integral–moment equations (3.1), (3.2). The approximating expressions (3.3) for the partial velocities $\bar{w}_i$, in particular, must be supplemented by $a_{3i}x^4$ terms.

The direction of the BLID surface component is determined by the signs of the difference between the accommodation coefficients of the unexcited and excited particles, $\Delta\varepsilon = \varepsilon_n - \varepsilon_m$, and the detuning of the radiation frequency from the center of the absorption line, $\Omega = \omega - \omega_{mn}$. If $\Delta\varepsilon > 0$, then the direction of the BLID surface component for $\Omega > 0$ coincides with the radiation direction, while for $\Omega < 0$ they are opposite.

It is seen from Table 1 that G_1 decreases monotonically in the transition from the free-molecule to the hydrodynamic regime. Such behavior is explained by the fact that the relative number of particles colliding with the channel walls decreases with increasing rarefaction δ. This weakens the role of the walls as a buffer, and G_1 decreases.

The dependence of the kinetic coefficient G_2, characterizing collisional BLID, on δ is nonmonotonic. That dependence has a maximum at $\delta \approx 4$, while G_2 changes sign at $\delta \approx 2$. This means that the direction of the BLID collisional component is determined not only by the signs of Ω and $\Delta\sigma/\sigma$ but also by the gas pressure in the channel.

The following is a possible reason for such a dependence of the function $G_2 = G_{2m} + G_{2n}$ on Kn. The components G_{2m} and G_{2n} for excited and unexcited particles are sign-constant functions of the Knudsen number, with $G_{2m} < 0$ and $G_{2n} > 0$. In the hydrodynamic regime, G_{2m} and G_{2n} are determined by kinetic processes in the Knudsen wall layer. The effective thickness of the Knudsen layer is greater for particles with a smaller collision cross section, such as those in the ground n-state. The flux J_n therefore encounters less channel resistance and $|G_{2n}| > |G_{2m}|$. With decreasing pressure, the thickness of the Knudsen layer increases and $|G_{2n}|$ and $|G_{2m}|$ increase, reaching maxima in the intermediate regime. A further pressure decrease leads to weakening of the BLID collisional mechanism itself, i.e., a decrease in $|G_{2m}|$ and $|G_{2m}|$, with $G_{2n}|$ decreasing faster. As a result, at some δ the macroscopic, oppositely directed fluxes of excited and unexcited particles turn out to be equal in magnitude. When this happens, the sign of G_2 changes. Then $|G_{2n}| < |G_{2m}|$ with increasing Knudsen number, i.e., $G_2 < 0$.

In Figs. 1 and 2 we give profiles of the dimensionless macroscopic velocities w_1 and w_2. It is seen (Fig. 1) that the BLID surface component w_1 at $\delta \geq 1$ hardly depends on the transverse coordinate. This suggests that the gas viscosity does not significantly affect the BLID surface component. We also note that at $\delta \leq 0.1$, the gas velocity w_1 is higher near the walls of the channel than at its axis.

The evolution of the profile of the velocity w_2 of the BLID collisional component with increasing rarefaction δ (Fig. 2) is interesting. So long as the rarefaction parameter is small, w_2 depends little on x. With increasing δ, the structure of the BLID flux becomes more complicated. A stream "core" moving in one direction is isolated near the channel axis while the part of the gas in the wall layer is moving in the opposite direction. The presence of counterflow is due to the fact that at intermediate δ, the flux of excited particles in the wall region is larger than the flux of unexcited particles, and vice versa near the axis. In the nearly free-molecule regime at $\delta \leq 0.1$, the gas velocity w_2 is in the opposite direction to the wave vector **k**. In the hydrodynamic regime at $\delta > 10$, the direction of w_2 coincides with that of **k** and w_2 increases with distance from the wall. The gas viscosity thus affects the BLID collisional velocity component w_2 at $\delta > 10$ in the wall layer.

The research described in this publication was made possible in part by Grant NRG 4000 from the International Science Foundation.

REFERENCES

1. F. Kh. Gel'mukhanov and A. M. Shalagin, "Light-induced gas diffusion," Pis'ma Zh. Eksp. Teor. Fiz., **29**, No. 12 (1979).
2. A. V. Chiner, M. I. Stockman, and M. A. Vaksman, "Surface light-induced drift of rarefied gas," Phys. Lett., **96A**, No. 2 (1983).
3. M. A. Vaksman and A. V. Gainer, "Theory of drift of a dense gas interacting with walls with velocity-selective excitation," Zh. Éksp. Teor. Fiz., **89**, No. 1(7) (1985).
4. I. V. Chermyaninov and V. G. Chernyak, "Gas slippage in an optical radiation field," Inzh.-Fiz. Zh., **55**, No. 6 (1988).
5. V. I. Roldugin, "Photoslippage of gas acted on by resonant radiation," Kolloid. Zh., **50**, No. 3 (1988).
6. F. É. Bazelyan and M. N. Kogan, "Light-induced drift of a one-component gas in a channel," Dokl. Akad. Nauk, **308**, No. 1 (1989).
7. S. G. Rautian, G. I. Smirnov, and A. M. Shalagin, Nonlinear Resonances in Atomic and Molecular Spectra [in Russian], Nauka, Novosibirsk (1979).
8. F. J. McCormack, "Construction of linearized kinetic models for gaseous mixtures and molecular gases," Phys. Fluids, **16**, No. 12 (1979).
9. I. V. Chermyaninov, V. G. Chernyak, and G. A. Fomyagin, "Accommodation dependence of heat and mass transfer of a polyatomic gas in a capillary at arbitrary Knudsen numbers," Teplofiz. Vys. Temp., **23**, No. 6 (1985).
10. G. J. Van der Meer, R. W. M. Hoogeveen, L. J. F. Hermans, and P. L. Chapovsky, "Light-induced drift of CH_3F in noble gases," Phys. Rev., **A39**, No. 10 (1989).

11. B. D. Fried and S. D. Conte, The Plasma Dispersion Function, Academic Press, New York (1961).
12. I. V. Chermyaninov and V. G. Chernyak, "Drift of a rarefied gas in a flat channel under the action of monochromatic radiation," Inzh.-Fiz. Zh., **60**, No. 6 (1991).
13. S. G. Mikhlin, Variational Methods in Mathematical Physics [in Russian], 2nd ed., Nauka, Moscow (1970) [1st ed. translated by T. Boddington, Macmillan, New York (1964)].
14. V. G. Chernyak, E. A. Vintovkina, and I. V. Chermyaninov, "Light-induced drift of a one-component gas in capillaries," Zh. Éksp. Teor. Fiz., **103**, No. 5 (1993).